Tunable HMF hydrogenation to furan diols in a flow reactor using Ru/C as catalyst

Fulignati, Sara; Antonetti, Claudia; Wilbers, Erwin; Licursi, Domenico; Heeres, Hero Jan; Raspolli Galletti, Anna Maria

Published in:
Journal of Industrial and Engineering Chemistry

DOI:
10.1016/j.jiec.2021.04.057

Publication date:
2021

Journal of Industrial and Engineering Chemistry 100 (2021) 390.e1–390.e9

Contents lists available at ScienceDirect

Journal of Industrial and Engineering Chemistry

journal homepage: www.elsevier.com/locate/jiec

Tunable HMF hydrogenation to furan diols in a flow reactor using Ru/C as catalyst

Sara Fulignati[a], Claudia Antonetti[a,b,*], Erwin Wilbers[c], Domenico Licursi[a], Hero Jan Heeres[c], Anna Maria Raspolli Galletti[a]

[a] Department of Chemistry and Industrial Chemistry, University of Pisa, Via G. Moruzzi 13, 56124, Pisa, Italy
[b] CIRCC, via Celso Ulpiani 27, 70126, Bari, Italy
[c] Green Chemical Reaction Engineering, ENTEG, University of Groningen, Nijenborgh 4, 9747 AG Groningen, The Netherlands

ARTICLE INFO

Article history:
Received 24 February 2021
Received in revised form 22 April 2021
Accepted 29 April 2021
Available online 4 May 2021

Keywords:
5-hydroxymethylfurfural
Tunable hydrogenation
Aqueous-phase
2,5-bis(hydroxymethyl)furan
2,5-bis(hydroxymethyl)tetrahydrofuran
Flow reactor

ABSTRACT

5-hydroxymethylfurfural (HMF), accessible from various feedstocks, represents an important renewable platform-chemical, precursor for valuable biofuels and bio-based chemicals. In this work, the continuous hydrogenation of an aqueous solution of HMF to give strategic monomers, 2,5-bis(hydroxymethyl)furan (BHMF) and 2,5-bis(hydroxymethyl)tetrahydrofuran (BHMTHF) was investigated in a continuous flow reactor adopting a commercial Ru/C (5 wt%) as catalyst. The influence of the main process variables on products yield and selectivity was studied and optimized. The highest BHMF and BHMTHF yields of 87.9 and 93.7 mol%, respectively, were achieved by tuning the catalyst contact time, keeping all other variables constant (temperature, pressure, hydrogen flow rate, initial HMF concentration). Intraparticle diffusion limitation for hydrogen and HMF was shown to occur at some of the tested conditions by performing the HMF hydrogenation with different catalyst particle sizes, confirmed by calculations. Constant catalyst activity was observed up to 6 h time-on-stream and then gradually reduced. Fresh and spent catalyst characterization showed no significant sintering and negligible leaching of ruthenium during time-on-stream. A decrease of the specific surface area was observed, mainly due to humin deposition which is likely the reason for catalyst deactivation. Catalyst performance could be restored to initial values by a thorough washing of the catalyst.

Introduction

The depletion of fossil resources together with their contribution to environmental issues related to CO_2 emissions have stimulated research towards the synthesis of chemicals from renewable resources, such as lignocellulosic biomasses [1]. In this regard, 5-hydroxymethylfurfural (HMF) is a key platform-chemical, accessible from monosaccharides and polysaccharides [2–9], and the precursor for several value-added products, such as 2,5-furandicarboxylic acid (FDCA), 2,5-dimethylfuran (DMF), 2,5-bis (hydroxymethyl)furan (BHMF), and 2,5-bis(hydroxymethyl)tetrahydrofuran (BHMTHF) [9–18].The two last compounds are obtained from the hydrogenation of the aldehyde group (BHMF) and also of the furanic ring (BHMTHF), as reported in Scheme 1.

Both are considered highly important intermediates due to their promising applications as valuable monomers [19] as well as precursors for other important monomers that, up to now, are obtained from fossil resources, such as caprolactam and 1,6-hexanediol [20–22]. Generally, HMF hydrogenations to BHMF and BHMTHF are carried out using heterogeneous catalysts, in particular noble metals supported on oxides, polymers, or carbon species, mainly tested in batch reactors [15,23–25]. However, this reactor set-up is not suitable for industrial applications where continuous operations are preferred [26–29]. Only recently, experimental studies using continuous set-ups have been reported for the synthesis of biobased chemicals [30], such as for the hydrogenation of levulinic acid [31–33], furfural [34–36] and HMF [22,37–48]. Regarding HMF hydrogenation in flow, the most investigated reaction involves the synthesis of DMF [37–45] and only limited researches deal with the synthesis of BHMF and BHMTHF [22,46–48]. An overview of the HMF hydrogenation carried out in flow reactors is given in Table 1.

Regarding the HMF hydrogenation to furan diols, Kumalaputri et al. carried out the hydrogenation of HMF to BHMF in ethanol employing Cu doped porous metal oxides (PMO) with an amount of Cu of 7.6 wt% (7.6 wt% Cu-PMO) as the catalyst [46]. At the

* Corresponding author.
E-mail address: claudia.antonetti@unipi.it (C. Antonetti).

https://doi.org/10.1016/j.jiec.2021.04.057
1226-086X/

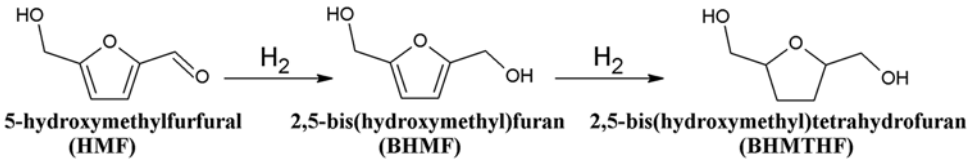

Scheme 1. Conversion of HMF to the desired products BHMF and BHMTHF.

Table 1
Overview of the literature on the HMF hydrogenation carried out in flow reactors.

Catalyst	Solvent	Reaction conditions	Catalyst contact time ($g_{cat} \times min/g_{HMF}$)	C_{HMF} (wt%)	HMF conversion (mol%)	Product yield (mol%)	Ref
15 wt% Ni/porous carbon	EtOH	150 °C 6 bar 30 ml/min H_2	50	0.6	79	68[a]	[37]
Ru/Cu/Fe_3O_4/N-rGO[b]	DMSO	150 °C 8 bar 47 ml/min H_2	1000	5.4	100	91[a]	[38]
0.7 wt% Pd/Al_2O_3	H_2O	189 °C 4 bar 50 ml/min H_2	400	5.0	100	13[a]	[39]
10 wt% Pt/C	1-PrOH	180 °C 33 bar 20 ml/min H_2	25	1.2	85	50[a]	[40]
15 wt% Cu/ZrO_2	1-BuOH	275 °C 15 bar n.a.[c]	400	1.5	100	26[a]	[41]
10 wt% Pt/C	EtOH	180 °C 33 bar 10 ml/min H_2	50	1.2	95	69[a]	[42]
10 wt% Pt_3Co_2/C	1-PrOH	160 °C 33 bar 5 ml/min H_2	100	1.2	100	98[a]	[43]
10 wt% Pt_3Ni/C	1-PrOH	200 °C 33 bar 5 ml/min H_2	100	1.2	100	98[a]	[44]
10 wt% $NiCu_3/C$	1-PrOH	180 °C 33 bar 3 ml/min H_2	175	1.2	100	98[a]	[45]
7.6 wt% Cu-PMO	EtOH	100 °C 50 bar 30 ml/min H_2	54	0.5	90	80[c]	[46]
5 wt% Cu/Al_2O_3 doped with 1.5 wt% K	EtOH	120 °C 20 bar 50 ml/min H_2	60	3.0	100	99[c]	[47]
RANEY Cu	H_2O	90 °C 90 bar n.a.[c]	280	1.0	n.a.[d]	86[c]	[48]
1) RANEY Cu 2) RANEY Ni	H_2O	90 °C 90 bar n.a.[c]	280	1.0	n.a.[d]	76[e]	[48]
0.6 wt% Pd/SiO_2	H_2O	100 °C 30 bar 60 ml/min H_2	1000	1.0	100	100[e]	[22]

[a] DMF.
[b] Bimetallic Ru and Cu loaded on N-doped reduced graphene oxide with iron oxide.
[c] BHMF.
[d] n.a. = not available.
[e] BHMTHF.

optimized reaction conditions, the BHMF yield of 80 mol% was reported together with the HMF conversion of 90 mol%. Hu et al. performed the same reaction in ethanol using a more concentrated HMF solution and 5 wt% Cu/Al_2O_3 doped with 1.5 wt% of potassium (to increase dispersion and reduce support acidity) as the catalyst [47]. Under the optimized conditions, the authors reported the BHMF yield of about 99 mol% at full HMF conversion. The hydrogenation of HMF to BHMF and BHMTHF in flow was investigated also in water, which is considered the most sustainable solvent in terms of toxicity and price. Lima et al. tested several commercial catalysts for the hydrogenation of HMF in an aqueous solution to BHMF and BHMTHF [48]. The authors found that RANEY Cu was the best catalyst for the synthesis of BHMF, affording the highest yield of 86 mol%, although interesting yields of BHMTHF (about 76 mol%) could be obtained only adopting a two-step procedure in which RANEY Cu was used in the first step for the hydrogenation of HMF to BHMF and RANEY Ni for the second step from BHMF to BHMTHF. In fact, the authors synthesized BHMTHF from the crude BHMF solution under the same reaction conditions of the first step, achieving the BHMTHF yield of 76 mol% respect to the starting HMF. Xiao et al. performed the synthesis of BHMTHF reaching quantitative yields from an aqueous HMF solution using 0.6 wt% Pd/SiO_2 as the catalyst [22].

We here report studies on BHMF and BHMTHF synthesis using aqueous HMF solutions as feed in a flow reactor. Instead of the most common organic solvents (tetrahydrofuran, 1,4-dioxane and alcohols) that allow high diols yields, in this work water was chosen as solvent. In fact, despite it generally promotes the formation of by-products like humins, it has a large number of benefits, being abundant, cheap, environmental compatible, non-toxic and non-flammable, making it preferable from a Green Chemistry point of view. On the basis of the above statements, HMF hydrogenation to diols in water is certainly challenging but also of great importance in order to develop a sustainable process for the synthesis of renewable monomers. For this reason several researches have recently investigated this reaction in water but most of them carried out it in batch and/or not optimizing the one-pot synthesis towards each diol [48–51]. On the contrary, and this is an absolute novelty of this paper, this research is focused on the possibility to achieve high yields of each diol in water without major modifications regarding process conditions. For this purpose, a commercial catalyst (5 wt% Ru/C), already successfully used by our research group in batch reactor, was employed [15,52,53]. As consequence, the process could become versatile and interesting under an industrial perspective because in this way it is made adaptable to the market request, reducing equipment, investment and production costs.

Experimental

Materials

HMF (99%) was supplied by Sigma-Aldrich. BHMF (98%) was purchased from Toronto Research Chemicals. BHMTHF (95%) was provided by GLSyntech. Ru/C (5 wt%), silicon carbide, and dichloromethane (99.9%) were purchased from Sigma-Aldrich. Milli-Q water was employed to prepare the solutions.

HMF hydrogenation in the flow reactor

The set-up of the flow reactor employed for HMF hydrogenation was composed of a feeding section, a preheater, a reactor (ID = 0.7 cm; L = 14.2 cm), a gas–liquid separator, and an auto-sampler (Scheme S1). In a standard run, the HMF aqueous solution was prepared adding 1, 5, 10 or 20 g of HMF to 1 l of water in order to obtain HMF concentration of 0.1, 0.5, 1.0 or 2.0 wt%, respectively. For the stability test, where the time-on-stream was up to 50 h, a larger amount of HMF solution was prepared and in this case 4 g of HMF were added to 4 l of water. The solution was then transferred in the feed vessel. The proper amount of catalyst (5 wt% Ru/C) and about 4 g of silicon carbide (inert filler) were loaded into the reactor. Subsequently, the reactor was closed and the HMF solution was fed through a piston pump with a volumetric feed flow rate of 1 ml/min. Catalyst contact times were varied by modifying the catalyst intake while keeping the volumetric feed flow rate constant. In particular, 0.01, 0.02, 0.05, 0.15 or 0.30 g of catalyst were loaded in the reactor in order to obtain the catalyst contact time of 10, 20, 50, 150 or 300 $g_{cat} \times min/g_{HMF}$, respectively. The pressure, monitored at two positions (before the preheater and immediately after the reactor), was set to the desired value, in the range of 10–50 bar, through a back pressure valve. The reactor and preheater were heated electrically to the pre-determined temperature, in the range of 60–120 °C, which was measured at the entrance and exit of the reactor through two thermocouples. Subsequently, the hydrogen flow, fed directly from the cylinder and changed in the range of 30–130 ml/min, was started and monitored by a flow controller. When the temperature reached the preset value, the reaction time was set to zero (t = 0 h). At different runtimes, liquid samples were collected by an in-house made auto-sampler and analysed by HPLC. The considered process variables and their ranges are summarized in Table 2.

Table 2
Process parameters and their values/ranges.

Process parameters	Units	Ranges
Liquid flow	ml/min	1
Catalyst contact time	$g_{cat} \times min/g_{HMF}$	10–300
Temperature	°C	60–120
Hydrogen pressure	bar	10–50
Hydrogen flow	ml/min	30–130
HMF inlet concentration	wt%	0.1–2.0
	mM	7.9–158.0
Time-on-stream	h	1–50

For the recycling tests, the employed catalyst was recovered from the reactor, washed three times under stirring with 5 ml of acetone at room temperature, filtered on a Gooch filtering crucible, dried in a vacuum oven at 40 °C overnight, and used in subsequent run.

Product analysis by HPLC

The liquid samples were filtered through a syringe filter (0.45 μm) and analyzed using an HPLC Agilent Technologies 1260 Infinity equipped with a Bio-Rad Aminex HPX-87H (300 × 7.8 mm) column kept at 60 °C, and employing 0.005 M H_2SO_4 as the mobile phase (flow rate: 0.55 ml/min). The concentrations of the products were determined from calibration curves obtained with standard solutions of different concentrations.

Product analysis by GC–MS

The products formed during the hydrogenation of HMF in flow were identified by gas chromatography coupled with a mass spectrometer (GC–MS). Before the analysis, 3 ml of the aqueous sample was extracted three times with 6 ml of dichloromethane under stirring, the organic phase was separated and collected together, concentrated by a rotary vacuum evaporator adopting the heating temperature of water bath of 50 °C until the volume was reduced by about a tenth. Finally, the concentrated solution was injected. A GC–MS (Hewlett Packard 5973-6890) equipped with a Restek RTX-1701 capillary column (30 m × 0.25 mm i.d. and 0.25 μm film 14%-cyanopropylphenyl/86%-dimethylpolysiloxane) was employed for the analysis. The temperatures of the injector and detector were set at 250 °C and 285 °C, respectively. The following temperature program was used: 40 °C isothermal for 10 min and then heating up with a heating rate of 10 °C/min up to 250 °C.

Catalyst characterization

Transmission Electron Microscopy (TEM) measurements in bright field mode were carried out with a CM12 microscope (Philips), operating at 120 keV. The catalysts were suspended in ethanol by ultra-sonication and the obtained sample was dropped onto carbon coated 400 mesh copper grids. Images were taken on a slow scanning CCD camera. The ruthenium particle size distribution was evaluated by measuring the particle diameter of at least 100 individual particles using Nano Measurer 1.2 software.

The surface area, pore volume and pore distribution of the fresh and spent catalysts were measured by means of nitrogen physisorption analyses performed using a Micromeritics ASAP 2020 at −196.2 °C. Before measurement, the samples (∼100 mg) were degassed under vacuum at 150 °C for 6 h. The surface area was estimated using the Barrett–Emmet–Taller (BET) method. The

cumulative pore volume, the average pore diameter and the pore size distribution were determined through the Barrett–Joyner–Halenda (BHJ) method.

Thermogravimetric analysis (TGA) of the fresh and spent catalysts was determined using a TGA Q50 system (TA Instrument). About 5 mg of the samples were heated in a nitrogen atmosphere in a temperature range between 20 and 650 °C adopting a heating rate of 10 °C/min.

The ruthenium content in the liquid sample collected at the end of the reaction was determined by inductively coupled plasma-optical emission spectrometry (ICP-OES) using an Optima 7000 DV (PerkinElmer) analyzer equipped with a CCD array detector and the wavelength used for Ru analysis was 240.27 nm.

Definitions

The HMF conversion ($Conversion_{HMF}$, mol%), and the yields of BHMF ($Yield_{BHMF}$, mol%) and BHMTHF ($Yield_{BHMTHF}$, mol%) were calculated according to Eqs. (1)–(3):

$$Conversion_{HMF} = \frac{C^{in}_{HMF} - C^{out}_{HMF}}{C^{in}_{HMF}} \times 100\% \quad (1)$$

$$Yield_{BHMF} = \frac{C^{out}_{BHMF}}{C^{in}_{HMF}} \times 100\% \quad (2)$$

$$Yield_{BHMTHF} = \frac{C^{out}_{BHMTHF}}{C^{in}_{HMF}} \times 100\% \quad (3)$$

where C^{in}_{HMF} is the inlet concentration of HMF (mol/l); C^{out}_{HMF}, C^{out}_{BHMF} and C^{out}_{BHMTHF} are the concentration of HMF, BHMF, and BHMTHF in the outlet flow (mol/l), respectively.

The carbon balance (mol%) was evaluated by comparing the sum of the molar concentration of unconverted HMF, the molar concentrations of products (BHMF and BHMTHF), and the molar concentrations of quantified by-products in the outlet flow with the starting concentration of HMF, according to Eq. (4):

$$Carbon\ \ balance = \frac{C^{out}_{HMF} + C^{out}_{BHMF} + C^{out}_{BHMTHF} + C^{out}_{others}}{C^{in}_{HMF}} \times 100\% \quad (4)$$

where C^{out}_{others} is the concentration of quantified by-products, in particular tetrahydrofurfuryl alcohol and 1,2-pentandiol, in the outlet flow (mol/l).

The catalyst contact time (CCT, $g_{cat} \times min/g_{HMF}$) was calculated according to Eq. (5):

$$CCT = \frac{m_{catalyst}}{\emptyset \times c_{HMF}} \quad (5)$$

where $m_{catalyst}$ is the amount (g) of the employed catalyst, $\emptyset$ is the volumetric flow rate of the feed (ml/min), and c_{HMF} is the concentration of HMF (g/ml) in the feed.

Results and discussion

Preliminary experiments of HMF hydrogenation in the flow reactor

Preliminary experiments (100 °C, 50 bar, CCT of 10 $g_{cat} \times min/g_{HMF}$, H_2 flow of 100 ml/min, liquid flow of 1 ml/min and HMF concentration of 0.1 wt% corresponding to 7.9 mM) were performed in triplicate in order to obtain information on the stability of the catalyst (5 wt% Ru/C) and the reproducibility of the experiments. The results for a 50 (A) and 6 h (B) time-on-stream experiment with the error bars are reported in Fig. 1.

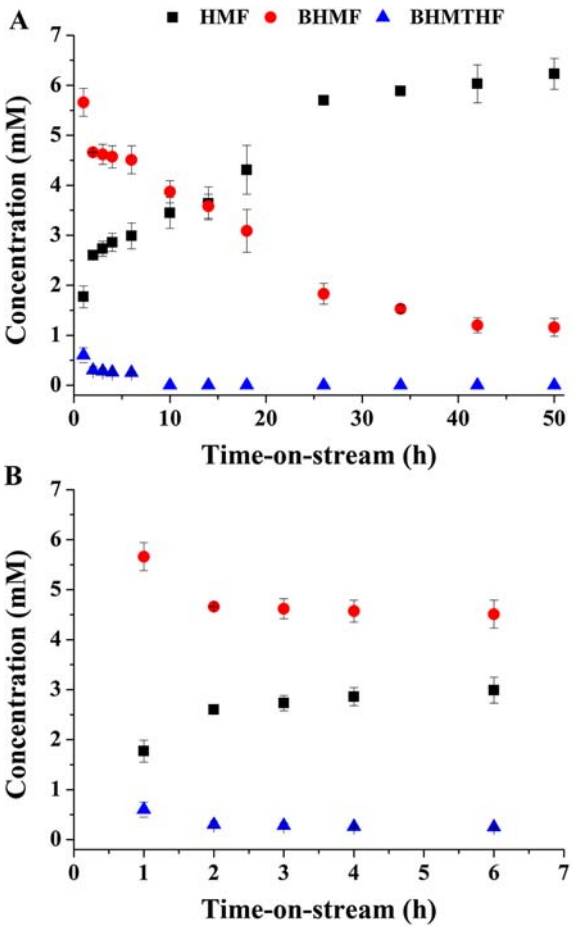

Fig. 1. Concentrations versus time-on-stream for the continuous HMF hydrogenation up to 50 h (A) and up to 6 h (B). Reaction conditions: T = 100 °C; P = 50 bar; [HMF] = 0.1 wt%; H_2 flow = 100 ml/min; liquid flow = 1 ml/min; catalyst contact time = 10 $g_{cat} \times min/g_{HMF}$. *Note*: where the error bars are not visible, they are smaller than the symbols.

Reproducibility was good and standard deviations in the HMF, BHMF, and BHMTHF concentrations were low (relative error of 7%). However, the concentration versus time curves indicate that catalyst stability was limited. In fact, high activity was found at the beginning of the reaction, followed by a small decay after 2 h. Subsequently, activity was almost constant between 2 and 6 h, followed by a decrease when prolonging the time-on-stream (Fig. 1A). For further experiments, the HMF conversion and product yields between 2 and 6 h were selected as being representative of the steady-state performance of the reactor (Fig. 1B). As such, the average HMF conversion and average yields of the products were calculated for the liquid samples collected between 2 and 6 h of time-on-stream at time lapses of 1 h. Under the reaction conditions employed in these preliminary experiments, the HMF conversion of 62.8 mol% was obtained with BHMF as the major product (58.5 mol% yield). BHMTHF was only obtained in low yield (1.8 mol %) together with trace amounts of other by-products (HPLC). After this preliminary study, the influence of the relevant reaction conditions on the selective synthesis of each diol was investigated in more detail.

Optimization of reaction parameters for the selective hydrogenation of HMF to a specific diol

The role of the CCT on catalyst performance was studied by performing the HMF hydrogenation with different catalyst intakes,

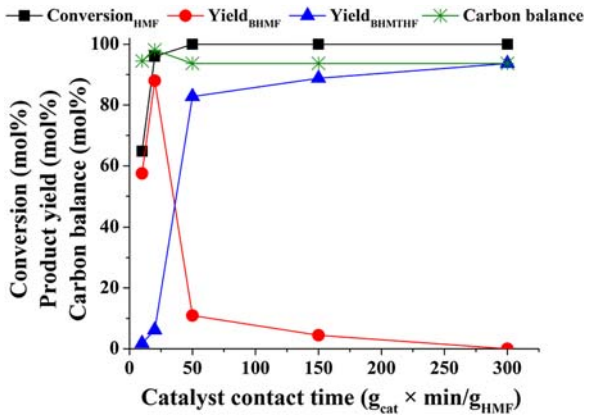

Fig. 2. Conversion, products yields and carbon balance versus catalyst contact time. Reaction conditions: T = 100 °C; P = 50 bar; [HMF] = 0.1 wt%; H_2 flow = 100 ml/min; liquid flow = 1 ml/min.

keeping the liquid flow rate constant (1 ml/min) and working at the same reaction conditions (100 °C, 50 bar, H_2 flow of 100 ml/min and the HMF feed concentration of 0.1 wt%). The results are provided in Fig. 2.

Complete HMF conversion was only possible when the CCT was larger than 50 g_{cat} × min/g_{HMF}. Moreover, at CCT values lower than 50 g_{cat} × min/g_{HMF} the main product was BHMF thus the selective hydrogenation of the aldehyde group was only possible at short contact times between the substrate and the catalyst. The highest BHMF yield of 88.0 mol% was obtained at 20 g_{cat} × min/g_{HMF}. At higher CCT values, hydrogenation of the furan ring occurred and the BHMTHF yield increased from 6.2 mol% at 20 g_{cat} × min/g_{HMF} to 93.7 mol% at 300 g_{cat} × min/g_{HMF}, which represents the highest value obtained in this study. The carbon balance ranged between 98.1 and 93.2 mol% and slightly decreased at higher CCT values. Thus, it can be concluded that the optimum CCT is 20 g_{cat} × min/g_{HMF} for the synthesis of BHMF and 300 g_{cat} × min/$g_{HMF}$for BHMTHF.

The effect of temperature (60–120 °C) on product selectivity and yield was studied at the above CCT values and the results are reported in Fig. 3.

Working at CCT of 20 g_{cat} × min/g_{HMF} (Fig. 3A), the HMF conversion versus temperature showed an optimum at 100 °C, reaching 96.0 mol%, whereas it decreased at 120 °C. Humins formation and their subsequent deposition on the catalyst surface, expected to be favoured at higher temperatures, may lead to pore blockage of the catalysts and therefore to a reduction in the overall rate. An increase of the extend of the humin formation rate at 120 °C was also confirmed by a reduction in the carbon balance closure (humins are not included, only water-soluble low molecular weight compounds, see Eq. (4)). A similar trend was found for the BHMF yield, which reached a maximum at 100 °C (88.0 mol%) and decreased at 120 °C. Moreover, when performing the reaction at 120 °C, traces of tetrahydrofurfuryl alcohol and 1,2-pentandiol were detected. These by-products derived from HMF decarbonylation to the intermediate furfuryl alcohol, which is known to be promoted at higher temperatures (Scheme S2) [39,54,55]. The successive hydrogenation of the furanic ring of furfuryl alcohol gives tetrahydrofurfuryl alcohol, which then undergoes the ring-opening reaction to 1,2-pentandiol [56]. Götz et al. and Wang et al. showed that furfuryl alcohol can also directly be converted to 1,2-pentandiol through a hydrogenolysis mechanism, for instance when using ruthenium catalysts in water [57,58]. Moreover, tetrahydrofurfuryl alcohol can be obtained from the C—C bond cleavage of BHMTHF (Scheme S2) [15,59].

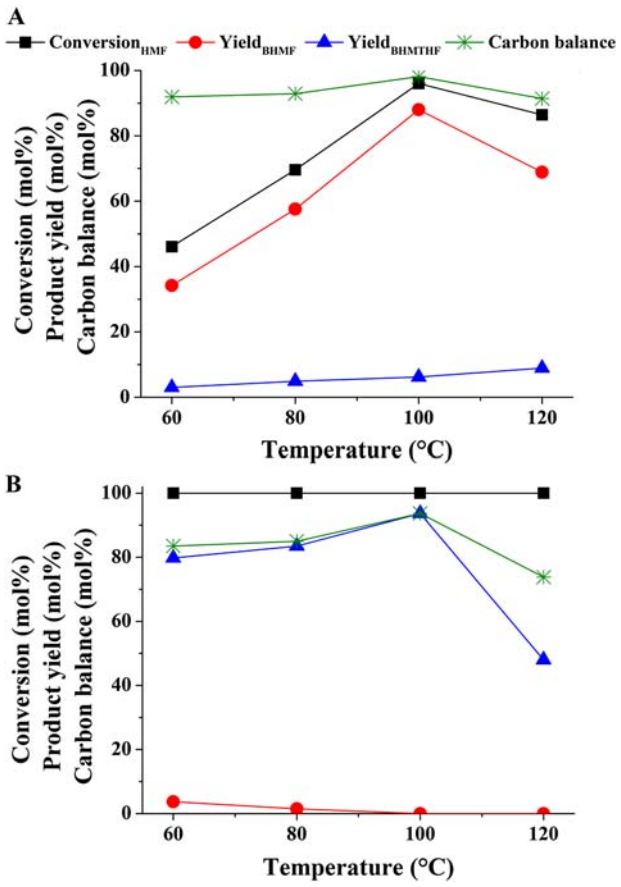

Fig. 3. Conversion, products yields and carbon balance versus temperature at catalyst contact time of 20 g_{cat} × min/g_{HMF} (A) and 300 g_{cat} × min/g_{HMF} (B). Reaction conditions: P = 50 bar; [HMF] = 0.1 wt%; H_2 flow = 100 ml/min; liquid flow = 1 ml/min.

When using a CCT value of 300 g_{cat} × min/g_{HMF} (Fig. 3B), quantitative HMF conversion was obtained at all temperatures in the range 60–120 °C. The BHMTHF yield showed a maximum value (93.7 mol%) at 100 °C. However, at 120 °C the BHMTHF yield markedly dropped, again likely due to humin formation. Also in this case, tetrahydrofurfuryl alcohol and 1,2-pentandiol were formed in yields of 14.8 and 11.2 mol%, respectively. Regarding the carbon balance, as expected it decreased when increasing the temperature from 100 to 120 °C, due to the formation of humins. However, both in Fig. 3A and B the carbon balance increased from 60 to 100 °C. A possible explanation is HMF adsorption on the catalyst surface [60], which leads to an overestimation of the HMF conversion. This hypothesis was proven by performing separate adsorption experiments of HMF (1 g/l) with Ru/C and SiC (room temperature, 20 min). Analysis of the mixtures showed that the HMF concentration was lower than the initial value for Ru/C (0.4 g/l), whereas the concentration was unchanged in the presence of SiC, thus confirming the high affinity of Ru/C for HMF.

The effect of the hydrogen pressure on HMF conversion and products yield when using CCT values of 20 g_{cat} × min/g_{HMF} (A) and 300 g_{cat} × min/g_{HMF} (B) at 100 °C are given in Fig. 4.

Only at the lowest CCT value an effect of hydrogen pressure on HMF conversion was observed and both the BHMF yield and HMF conversion increased at higher pressures (10–50 bar, Fig. 4A). At the higher CCT value (Fig. 4B), the HMF conversion was complete already at 10 bar. At higher pressures, hydrogenation of the furan ring of BHMF was promoted giving BHMTHF as the major product (93.7 mol% at 50 bar). Moreover, Fig. 4 shows that the carbon balance closure was only slightly reduced at higher pressures,

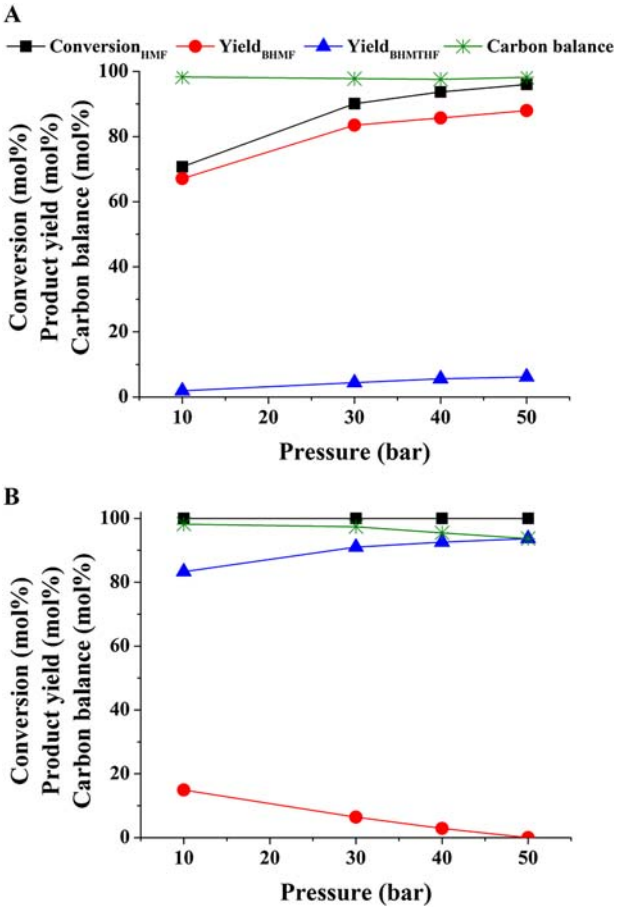

Fig. 4. Conversion, products yields and carbon balance versus pressure at a catalyst contact time of 20 $g_{cat} \times min/g_{HMF}$ (A) and 300 $g_{cat} \times min/g_{HMF}$ (B). Reaction conditions: T = 100 °C; [HMF] = 0.1 wt%; H_2 flow = 100 ml/min; liquid flow = 1 ml/min.

indicating that by-product formation is not markedly influenced by this parameter.

Analogous trends were also found when investigating the influence of the hydrogen flow rate (Fig. S1). In this case, a flow of 100 ml/min gave the best results for each diol. For all experiments, hydrogen was present in molar excess with respect to HMF, and as such an effect of hydrogen flow rate on catalyst performance is not expected. Thus, it more likely that this is due to mass transfer issues when working at low hydrogen flow rates due to negative effects on the volumetric mass transfer coefficients [61].

In conclusion, the selective hydrogenation of HMF to either BHMF or BHMTHF in a flow reactor with the same commercial catalyst Ru/C was demonstrated for the first time and their yields were optimized [22,46–48]. Moreover, the selectivity to either BHMF or BHMTHF resulted tunable with the CCT, keeping all other reaction conditions constant (temperature, pressure, and hydrogen flow rate).

Effect of HMF feed concentration

From an economic perspective, it is advantageous to work at the highest possible HMF feed concentrations, as this will reduce purification and solvent recycle costs and increase the process productivity (kg product/$m^3 \times h$). Therefore, the syntheses of BHMF and BHMTHF were carried out under the respective best reaction conditions identified in the previous paragraph employing higher feed concentrations of HMF (max 2.0 wt%).

In both cases, higher HMF feed concentrations had a negative effect on conversion and product selectivity. For BHMF synthesis (Fig. 5A), an increase in HMF feed concentration led to a marked drop in HMF conversion and BHMF yield, from 88.0 mol% at the HMF feed concentration of 0.1 wt% to 17.5 mol% at 2.0 wt%. This is likely due to a combination of a short contact time between the substrate and the active sites and a higher formation rate of humins promoted at higher HMF concentrations [62], confirmed by a reduction in the carbon balance closure. A similar trend was found when using process conditions optimal for BHMTHF synthesis (Fig. 5B). Besides, by-products, such as 1,2-pentandiol and tetrahydrofurfuryl alcohol, were detected in yields of about 4.0 and 3.0 mol%, respectively. Moreover, other not quantified soluble by-products were detected and identified by GC—MS analysis. Examples are furfuryl alcohol, 1,5-pentanediol, 1,2,6-hexanetriol, tetrahydropyran-2-methanol, 1,2-hexanediol, and 1,5-hexanediol. These can originate from the decomposition/hydrogenation of HMF and BHMTHF (Scheme S3). For instance as previously reported, tetrahydrofurfuryl alcohol can be formed by C—C bond cleavage of BHMTHF [59] and the hydrogenation of furfuryl alcohol, originating from HMF decarbonylation [54,55]. Both furfuryl alcohol and tetrahydrofurfuryl alcohol can undergo the ring-opening reaction leading to 1,2-pentandiol and/or 1,5-pentandiol [56,63–65]. On the other hand, also BHMTHF is prone to ring-opening reactions leading, in this case, to 1,2,6-hexanetriol [15,56,65–67], which can be converted to tetrahydropyran-2-methanol [20,66,67] or 1,2-hexanediol and 1,5-hexanediol,

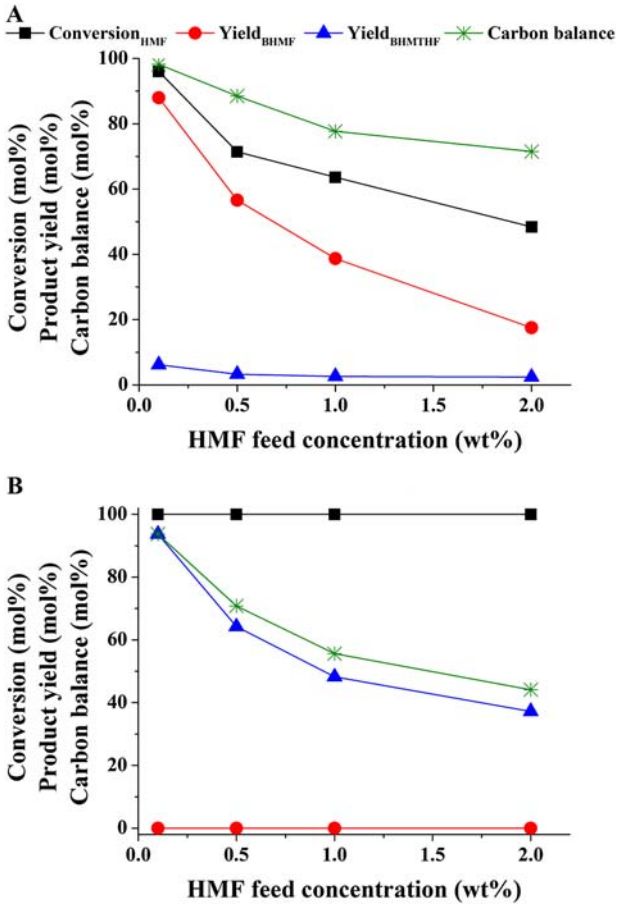

Fig. 5. Conversion, products yields and carbon balance versus HMF feed concentration with a catalyst intake of 0.02 g (A) and 0.30 g (B). Reaction conditions: T = 100 °C; P = 50 bar; H_2 flow = 100 ml/min; liquid flow = 1 ml/min.

through hydrogenolysis of the C—O bond [53,65,66]. Thus, when using a more concentrated HMF feed, condensation reactions to give humins as well as by-product formation reduce the chemoselectivity to the desired diols.

Internal mass transfer effects

HMF hydrogenation using a solid catalyst involves three phases system and thus the observed rate is determined by the intrinsic reaction rate and the rate of mass transfer of hydrogen and/or HMF to the active sites of the catalyst. In particular, both external mass transfer, responsible for the transport of soluble reagents in the liquid phase to the surface of the catalyst, and internal mass transfer, responsible for intraparticle transport, may limit the rate of the overall reaction. Here, we have considered only the effect of intraparticle mass transfer on the overall reaction rate, as it is typically the most limiting for heterogeneous reaction systems [68]. Possible intraparticle mass transfer limitations of hydrogen and HMF were estimated using the Weisz–Prater criterium (Eq. (6)) [69].

$$N_{W-P} = \frac{-R_{exp} \times r_p^2}{C_s \times D_{eff}} \quad (6)$$

Here, R_{exp} is the experimentally observed reaction rate (mol/$m^3_{cat} \times s$); r_p is the radius of catalyst particle (m); C_s is the concentration of the component at the catalyst surface (mol/m^3), D_{eff} is the effective diffusion coefficient of the component (m^2/s) and their expressions are reported in the Supplementary Data. In case the Weisz–Prater number is below 0.3, intraparticle mass transfer limitation of reagents is negligible. We have evaluated the Weisz–Prater number for all experiments and the details are provided in the Supplementary data (Tables S1 and S2). Intraparticle mass transfer limitations were shown to be relevant for HMF and, in a few runs, also for hydrogen. Experimental confirmation for intraparticle mass transfer limitations was obtained by performing the reaction with Ru/C samples having different average particle sizes. For this purpose, the catalyst was sieved into two fractions, one having particles in the range of 25–75 μm and the second one with particles in the range of 150–200 μm. The two fractions were employed at the same reaction conditions used for the experiment reported in Fig. 1 and the results are shown in Fig. 6.

The use of the smaller catalyst particles gave an improvement of HMF conversion of about 46.8 mol% respect to the larger ones, confirming that intraparticle mass transfer limitations affect the overall rates and thus the conversion/yield versus time-on-stream profiles. Such intraparticle mass transfer limitations have also been reported in the literature for several hydrogenations of biobased platform chemicals using Ru-based catalysts. Moreno-Marrodan et al. obtained a 10 mol% higher LA conversion when the average particle size of a Ru/DOWEX 50WX2 catalyst was decreased from 276 to 84 μm [70], whereas Piskun et al. reported an improvement of 34 mol% for the LA conversion when a millimeter-sized Ru/C catalyst (1.25–2.50 mm) was crushed and sieved in a fraction having particle sizes between 0.5 and 0.6 mm [32]. More recently, Hommes et al. employed two different Ru/C particle sizes (0.45 and 0.30 mm) for the hydrogenation of LA to GVL in a packed bed reactor and carried out the reaction at different CCT founding that both LA conversion and GVL yield were higher for a certain CCT when smaller catalysts particles were employed [71].

Catalyst stability and recyclability

The catalytic activity was shown to decrease during extended time-on-stream (Fig. 1, 50 h). The spent catalyst recovered from this experiment was characterized in details to get a better understanding of the deactivation mechanism. The surface area of the spent catalyst (136 m^2/g) was significantly lower than that of the fresh one (770 m^2/g). As ascertained in previous work [15], this is likely due to the deposition of humins and other compounds, such as HMF, on the catalyst surface that results in pore blockage. This is also evident from the pore size distributions of the fresh and spent catalysts (Fig. 7).

In fact, the corresponding pore size distributions derived by the Barrett–Joyner–Halenda (BJH) model show a higher amount of small pores, having a pore diameter of around 38 Å, for the fresh catalyst. After the reaction, these pores are extensively blocked by the deposition of humins, thus their amount decreases and larger pores become more relevant. As a consequence, the spent catalyst is characterized by lower pore volume and higher pore diameter respect to the fresh catalyst, being respectively the cumulative pore volume 0.39 and 0.46 cm^3/g and the average pore diameter 120.2 and 64.4 Å. Another proof of the presence of humins on the spent catalyst surface is given by the TGA analysis reported in Fig. 8.

In fact, it shows that the spent catalyst has more weight loss than the fresh catalyst due to the presence of carbonaceous material adsorbed on the catalyst surface, as already reported in the literature [17,72]. TEM analysis was carried out on the spent catalyst to verify the occurrence of ruthenium particle sintering. TEM micrographs and the ruthenium particles distributions for the

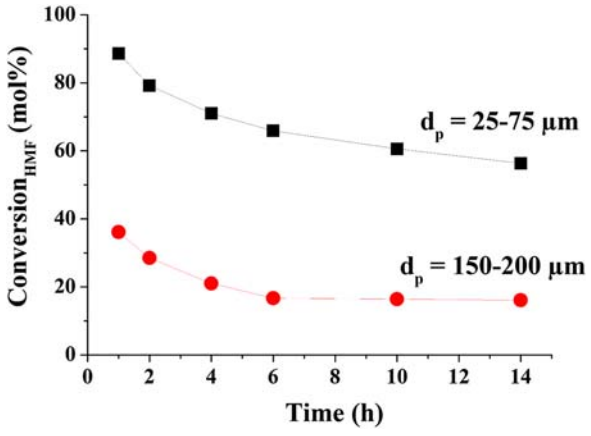

Fig. 6. Conversion in the presence of different catalyst particle sizes: 25–75 μm and 150–200 μm. Reaction conditions: catalyst contact time = 10 $g_{cat} \times min/g_{HMF}$; T = 100 °C; P = 50 bar; H_2 flow = 100 ml/min; liquid flow = 1 ml/min.

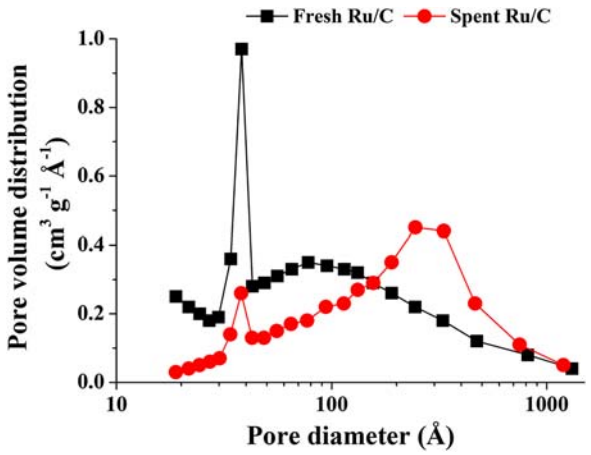

Fig. 7. Pore size distributions for fresh and spent 5 wt% Ru/C employed in the experiment of Fig. 1.

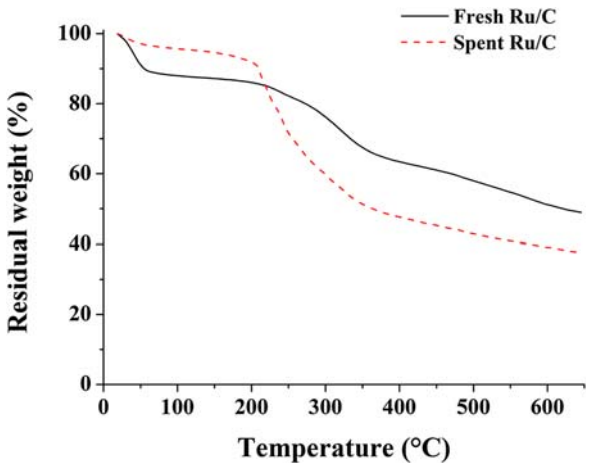

Fig. 8. Thermogravimetric curves of fresh and spent 5 wt% Ru/C employed in the experiment of Fig. 1.

fresh Ru/C and the spent Ru/C catalysts are provided in Fig. S2. The fresh Ru/C catalyst was characterized by an average ruthenium particle size of 1.5 nm, in agreement with the results reported in the literature [73,74]. In the spent catalyst, some sintering was detected and the average ruthenium particle size increased up to 2.5 nm, in line with the Ru nanoparticle size of the spent catalyst recovered from batch hydrogenation of HMF [15]. It has been shown that water can facilitate Ru particle agglomeration and that this process already occurs at room temperature [75,76]. Leaching of ruthenium from the catalyst was also investigated through ICP analysis by determination of the Ru content in the liquid samples obtained during run reported in Fig. 1. In all samples, the amount of ruthenium was below the detection limit, indicating that leaching of Ru was negligible.

These results indicate that deactivation of the catalyst during the time-on-stream is most likely related to the humin deposition on the surface. To verify whether this process is reversible, the spent catalyst was removed from the reactor, washed under stirring with acetone, filtered, dried under vacuum at 40 °C, and re-used in a subsequent run under the same reaction conditions of the experiment reported in Fig. 1 (100 °C, 50 bar, 0.1 wt% of HMF, H_2 flow of 100 ml/min and liquid flow of 1 ml/min). The same procedure was adopted for a second recycle. The results of these recycling experiments are given in Fig. 9.

It is evident that an acetone wash led to a performance close to that found for the fresh catalyst. This confirms that deposition of humins and other compounds is most likely the major deactivation mechanism, whilst the slight increase in the ruthenium particle sizes does not affect the catalytic activity, as already indicated by previous works [15,52,53]. Besides, TEM analyses of the catalysts at the end of the first and second recycle did not show an appreciable increase in the average Ru nanoparticle size. In this regard, the washing reactivation procedure can be extended also to the catalysts recovered from the reactions optimised for the synthesis of BHMF and BHMTHF, which were carried out under the same reaction conditions but at different CCT, a parameter that does not significantly influence the humins formation as evidenced by the almost analogous trend of carbon balance (Fig. 2).

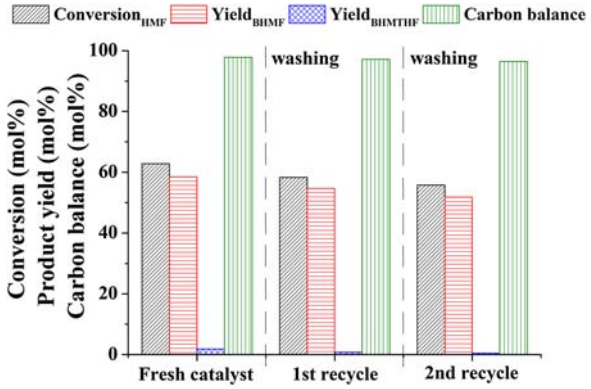

Fig. 9. HMF conversion, products yields and carbon balance in the presence of the fresh catalyst and after two recycles. Reaction conditions: catalyst contact time = 10 $g_{cat} \times min/g_{HMF}$T = 100 °C; P = 50 bar; [HMF] = 0.1 wt%; H_2 flow = 100 ml/min; liquid flow = 1 ml/min.

Conclusions

We here report the selective hydrogenation of HMF to either 2,5-bis(hydroxymethyl)furan (BHMF) or 2,5-bis(hydroxymethyl) tetrahydrofuran (BHMTHF) in a continuous flow reactor using a commercial 5 wt% Ru/C catalyst in water. The influence of relevant reaction parameters for the selective synthesis of one of the diols was determined and optimized. The highest BHMF and BHMTHF yields of 88.0 and 93.7 mol%, respectively, were obtained by tuning the catalyst contact time (CCT), keeping all other reaction parameters at the same values. This approach is very promising from an application perspective, because the CCT can be easily modified by changing the adopted feed flow, thus allowing for the selective synthesis of each diol without changing the type of catalyst and reaction conditions. TEM, ICP and nitrogen physisorption analyses proved that the experimentally observed deactivation of the catalyst after extended runtimes (>6 h) was mainly due to the deposition of humins on the catalyst surface. However, recycle experiments showed that the catalyst can be efficiently reactivated by an acetone wash.

Declaration of interests

The authors declare that they have no known competing financial interests or personal relationships that could have appeared to influence the work reported in this paper.

Declaration of Competing Interest

The authors report no declarations of interest.

Acknowledgments

The project PRA_2018_26 of University of Pisa is gratefully acknowledged.

Appendix A. Supplementary data

Supplementary material related to this article can be found, in the online version, at doi:https://doi.org/10.1016/j.jiec.2021.04.057.

References

[1] R.A. Sheldon, ACS Sustain. Chem. Eng. 6 (2018) 4464, doi:http://dx.doi.org/10.1021/acssuschemeng.8b00376.
[2] C. Antonetti, M. Melloni, D. Licursi, S. Fulignati, E. Ribechini, S. Rivas, J.C. Parajó, F. Cavani, A.M. Raspolli Galletti, Appl. Catal. B Environ. 206 (2017) 364, doi:http://dx.doi.org/10.1016/j.apcatb.2017.01.056.
[3] C. Antonetti, A.M. Raspolli Galletti, S. Fulignati, D. Licursi, Catal. Commun. 97 (2017) 146, doi:http://dx.doi.org/10.1016/j.catcom.2017.04.032.
[4] A. Sarwono, Z. Man, A. Idris, A.S. Khan, N. Muhammad, C.D. Wilfred, J. Ind, Eng. Chem. 69 (2019) 171, doi:http://dx.doi.org/10.1016/j.jiec.2018.09.020.
[5] G. Portillo Perez, A. Mukherjee, M.-J. Dumont, J. Ind. Eng. Chem. 70 (2019) 1, doi:http://dx.doi.org/10.1016/j.jiec.2018.10.002.
[6] C. Antonetti, S. Fulignati, D. Licursi, A.M. Raspolli Galletti, ACS Sustain. Chem. Eng. 7 (2019) 6830, doi:http://dx.doi.org/10.1021/acssuschemeng.8b06162.

[7] C. Sonsiam, A. Kaewchada, S. Pumrod, A. Jaree, Chem. Eng. Process. 138 (2019) 65, doi:http://dx.doi.org/10.1016/j.cep.2019.03.001.
[8] H.B. Phan, Q.B.T. Nguyen, C.M. Luong, K.N. Tran, P.H. Tran, Mol. Catal. 503 (2021) 111428, doi:http://dx.doi.org/10.1016/j.mcat.2021.111428.
[9] Q. Hou, X. Qi, M. Zhen, H. Qian, Y. Nie, C. Bai, S. Zhang, X. Bai, M. Ju, Green Chem. 23 (2021) 119, doi:http://dx.doi.org/10.1039/d0gc02770g.
[10] H. Liu, X. Cao, T. Wang, J. Wei, X. Tang, X. Zeng, Y. Sun, T. Lei, S. Liu, L. Lin, J. Ind. Eng. Chem. 77 (2019) 209, doi:http://dx.doi.org/10.1016/j.jiec.2019.04.038.
[11] S. Saxena, D. Yadaw, K. Tiwari, V. Venkatesh, S. Verma, R.G.S. Pala, S. Sivakumar, Catal. Lett. 151 (2021) 921, doi:http://dx.doi.org/10.101007/s10562-020-03361-1.
[12] N. Ma, Y. Song, F. Han, G.I.N. Waterhouse, Y. Li, S. Ai, Catal. Sci. Technol. 10 (2020) 4010, doi:http://dx.doi.org/10.1039/D0CY00363H.
[13] X. Wang, X. Liang, J. Li, Q. Li, Appl. Catal. A Gen. 576 (2019) 85, doi:http://dx.doi.org/10.1016/j.apcata.2019.03.005.
[14] D. Wu, S. Zhang, W.Y. Hernández, W. Baaziz, O. Ersen, M. Marinova, A.Y. Khodakov, V.V. Ordomsky, ACS Catal. 11 (2021) 19, doi:http://dx.doi.org/10.1021/acscatal.0c03955.
[15] S. Fulignati, C. Antonetti, D. Licursi, M. Pieraccioni, E. Wilbers, H.J. Heeres, A.M. Raspolli Galletti, Appl. Catal. A Gen. 578 (2019) 122, doi:http://dx.doi.org/10.1016/j.apcata.2019.04.007.
[16] T. Wang, J. Wei, H. Liu, Y. Feng, X. Tang, X. Zeng, Y. Sun, T. Lei, L. Lin, J. Ind, Eng. Chem. 81 (2020) 93, doi:http://dx.doi.org/10.1016/j.jiec.2019.08.057.
[17] J. Zhang, T. Wang, X. Tang, L. Peng, J. Wei, L. Lin, Bioresources 13 (2018) 7137, doi:http://dx.doi.org/10.15376/biores.13.3.Zhang.
[18] W.R. Silva, E.Y. Matsubatra, J.M. Rosolen, P.M. Donate, R. Gunnella, Mol. Catal. 504 (2021) 111496, doi:http://dx.doi.org/10.1016/j.mcat.2021.111496.
[19] D. Maniar, Y. Jiang, A.J.J. Woortman, J. Van Dijken, K. Loos, ChemSusChem 12 (2019) 990, doi:http://dx.doi.org/10.1002/cssc.201802867.
[20] J.G. De Vries, T. Buntara, P.H. Phua, I.V. Melián-Cabrera, H.J. Heeres, US9199961B2 (2015).
[21] H. Kim, S. Lee, W. Won, Energy 214 (2021) 118974, doi:http://dx.doi.org/10.1016/j.energy.2020.118974.
[22] B. Xiao, M. Zheng, X. Li, J. Pang, R. Sun, H. Wang, X. Pang, A. Wang, X. Wang, T. Zhang, Green Chem. 18 (2016) 2175, doi:http://dx.doi.org/10.1039/C5GC02228B.
[23] D.K. Mishra, H.J. Lee, C.C. Truong, J. Kim, J. Suh, Y.W. Baek, Y.J. Kim, Mol. Catal. 484 (2020) 110722, doi:http://dx.doi.org/10.1016/j.mcat.2019.110722.
[24] K.T.V. Rao, Y. Hu, Z. Yuan, Y. Zhang, C.C. Xu, Appl. Catal. A Gen. 609 (2021) 117892, doi:http://dx.doi.org/10.1016/j.apcata.2020.117892.
[25] E. Soszka, M. Jędrzejczyk, I. Kocemba, N. Keller, A.M. Ruppert, Catalysts 10 (2020) 1026, doi:http://dx.doi.org/10.3390/catal10091026.
[26] S. Han, M.A. Kashfipour, M. Ramezani, M. Abolhasani, Chem. Commun. 56 (2020) 10593, doi:http://dx.doi.org/10.1039/d0cc03511d.
[27] F.M. Akwi, P. Watts, Chem. Commun. 54 (2018) 13894, doi:http://dx.doi.org/10.1039/C8CC07427E.
[28] N. Kockmann, P. Thenée, C. Fleischer-Trebes, G. Laudadio, T. Noël, React. Chem. Eng. 2 (2017) 258, doi:http://dx.doi.org/10.1039/C7RE00021A.
[29] P.D. Morse, R.L. Beingessner, T.F. Jamison, Isr. J. Chem. 57 (2017) 218, doi:http://dx.doi.org/10.1002/ijch.201600095.
[30] A. Hommes, H.J. Heeres, J. Yue, ChemCatChem 11 (2019) 4671, doi:http://dx.doi.org/10.1002/cctc.201900807.
[31] M. Kondeboina, S.S. Enumula, K.S. Reddy, P. Challa, D.R. Burri, S.R.R. Kamaraju, Fuel 285 (2021) 119094, doi:http://dx.doi.org/10.1016/j.fuel.2020.119094.
[32] A.S. Piskun, J.E. De Haan, E. Wilbers, H.H. Van de Bonekamp, Z. Tang, H.J. Heeres, ACS Sustain. Chem. Eng. 4 (2016) 2939, doi:http://dx.doi.org/10.1021/acssuschemeng.5b00774.
[33] B. Mallesham, P. Sudarsanam, B.V.S. Reddy, B.G. Rao, B.M. Reddy, ACS Omega 3 (2018) 1639, doi:http://dx.doi.org/10.1021/acsomega.8b02008.
[34] H.R. Prakruthi, B.M. Chandrashekara, B.S. Jai Prakash, Y.S. Bhat, J. Ind. Eng. Chem. 62 (2018) 96, doi:http://dx.doi.org/10.1016/j.jiec.2017.12.048.
[35] M. Pirmoradi, N. Janulaitis, R.J. Gulotty, J.R. Kastner, Ind. Eng. Chem. Res. 59 (2020) 17748, doi:http://dx.doi.org/10.1021/acs.iecr.0c02866.
[36] R. Huang, Q. Cui, Q. Yuan, H. Wu, Y. Guan, P. Wu, ACS Sustain. Chem. Eng. 6 (2018) 6957, doi:http://dx.doi.org/10.1021/acssuschemeng.8b00801.
[37] C.M. Mani, M. Braun, V. Molinari, M. Antonietti, N. Fechler, ChemCatChem 9 (2017) 3388, doi:http://dx.doi.org/10.1002/cctc.201700506.
[38] G.Y. Jeong, A.K. Singh, S. Sharma, K.W. Gyak, R.A. Maurya, D.P. Kim, NPG Asia Mater. 7 (2015)e173, doi:http://dx.doi.org/10.1038/am.2015.21.
[39] D.P. Duarte, R. Martínez, L.J. Hoyos, Ind. Eng. Chem. Res. 55 (2016) 54, doi:http://dx.doi.org/10.1021/acs.iecr.5b02851.
[40] J. Luo, L. Arroyo-Ramírez, J. Wei, H. Yun, C.B. Murray, R.J. Gorte, Appl. Catal. A Gen. 508 (2015) 86, doi:http://dx.doi.org/10.1016/j.apcata.2015.10.009.
[41] N. Viar, J.M. Requies, I. Agirre, A. Iriondo, P.L. Arias, Energy 172 (2019) 531, doi:http://dx.doi.org/10.1016/j.energy.2019.01.109.
[42] J. Luo, L. Arroyo-Ramìrez, R.J. Gorte, D. Tzoulaki, D.G. Vlachos, AIChE J. 61 (2015) 590, doi:http://dx.doi.org/10.1002/aic.14660.
[43] J. Luo, H. Yun, A.V. Mironenko, K. Goulas, J.D. Lee, M. Monai, C. Wang, V. Vorotnikov, C.B. Murray, D.G. Vlachos, P. Fornasiero, R.J. Gorte, ACS Catal. 6 (2016) 4095, doi:http://dx.doi.org/10.1021/acscatal.6b00750.
[44] J. Luo, J.D. Lee, H. Yun, C. Wang, M. Monai, C.B. Murray, P. Fornasiero, R.J. Gorte, Appl. Catal. B Environ. 199 (2016) 439, doi:http://dx.doi.org/10.1016/j.apcatb.2016.06.051.
[45] J. Luo, M. Monai, C. Wang, J.D. Lee, T. Duchoň, F. Dvořák, V. Matolín, C.B. Murray, P. Fornasiero, R.J. Gorte, Catal. Sci. Technol. 7 (2017) 1735, doi:http://dx.doi.org/10.1039/c6cy2647h.
[46] A.J. Kumalaputri, G. Bottari, P.M. Erne, H.J. Heeres, K. Barta, ChemSusChem 7 (2014) 2266, doi:http://dx.doi.org/10.1002/cssc.201402095.
[47] D. Hu, H. Hu, H. Zhou, G. Li, C. Chen, J. Zhang, Y. Yang, Y. Hu, Y. Zhang, L. Wang, Catal. Sci. Technol. 8 (2018) 6091, doi:http://dx.doi.org/10.1039/C8CY02017E.
[48] S. Lima, D. Chadwick, K. Hellgardt, RSC Adv. 7 (2017) 31401, doi:http://dx.doi.org/10.1039/C7RA03318D.
[49] W.R. Silva, E.Y. Matsubara, J.M. Rosolen, P.M. Donate, R. Gunnella, Mol. Catal. 504 (2021) 111496, doi:http://dx.doi.org/10.1016/j.mcat.2021.111496.
[50] J. Tan, J. Cui, Y. Zhu, X. Cui, Y. Shi, W. Yan, Y. Zhao, ACS Sustain. Chem. Eng. 7 (2019) 10670, doi:http://dx.doi.org/10.1021/acssuschemeng.9b01327.
[51] C. Chen, R. Fan, W. Gong, H. Zhang, G. Wang, H. Zhao, Dalton Trans. 47 (2018) 17276, doi:http://dx.doi.org/10.1039/c8dt03907k.
[52] D. Licursi, C. Antonetti, S. Fulignati, M. Giannoni, A.M. Raspolli Galletti, Catalysts 8 (2018) 277, doi:http://dx.doi.org/10.3390/catal8070277.
[53] S. Rivas, A.M. Raspolli Galletti, C. Antonetti, D. Licursi, V. Santos, J.C. Parajó, Catalysts 8 (2018) 169, doi:http://dx.doi.org/10.3390/catal8040169.
[54] Q. Meng, D. Cao, G. Zhao, C. Qiu, X. Liu, X. Wen, Y. Zhu, Y. Li, Appl. Catal. B Environ. 212 (2017) 15, doi:http://dx.doi.org/10.1016/apcatb.2017.04.069.
[55] N. An, D. Ainembabazi, C. Reid, K. Samudrala, K. Wilson, A.F. Lee, A. Voutchkova-Kostal, ChemSusChem 13 (2020) 312, doi:http://dx.doi.org/10.1002/cssc.201901934.
[56] K. Tomishige, Y. Nakagawa, M. Tamura, Green Chem. 19 (2017) 2876, doi:http://dx.doi.org/10.1039/C7GC00620A.
[57] D. Götz, M. Lucas, P. Claus, React. Chem. Eng. 1 (2016) 161, doi:http://dx.doi.org/10.1039/C5RE00026B.
[58] X. Wang, Y. Weng, X. Zhao, X. Xue, S. Meng, Z. Wang, W. Zhang, P. Duan, Q. Sun, Y. Zhang, Ind. Eng. Chem. Res. 59 (2020) 17210, doi:http://dx.doi.org/10.1021/acs.iecr.0c01023.
[59] Y. Yang, Z. Du, J. Ma, F. Lu, J. Zhang, J. Xu, ChemSusChem 7 (2014) 1352, doi:http://dx.doi.org/10.1002/cssc.201301270.
[60] R.R. Gonzales, Y. Hong, J.H. Park, G. Kumar, S.H. Kim, J. Chem. Technol. Biotechnol. 91 (2016) 1157, doi:http://dx.doi.org/10.1002/jctb.4701.
[61] N. Al-Raifi, F. Galvanin, M. Morad, E. Cao, S. Cattaneo, M. Sankar, V. Dua, G. Hutchings, A. Gavriilidis, Chem. Eng. Sci. 149 (2016) 129, doi:http://dx.doi.org/10.1016/j.ces.2016.03.018.
[62] Z. Cheng, K.A. Goulas, N.Q. Rodriguez, B. Saha, D.G. Vlachos, Green Chem. 22 (2020) 2301, doi:http://dx.doi.org/10.1039/c9gc03961a.
[63] B. Kuang, Q. Zhang, Y. Fang, Y. Bai, S. Qiu, P. Wu, Y. Qin, T. Wang, Ind. Eng. Chem. Res. 59 (2020) 9372, doi:http://dx.doi.org/10.1039/C7GC00620A.
[64] T.P. Sulmonetti, B. Hu, S. Lee, P.K. Agrawal, C.W. Jones, ACS Sustain. Chem. Eng. 5 (2017) 8959, doi:http://dx.doi.org/10.1021/acssuschemeng.7b01769.
[65] A. Iriondo, I. Agirre, N. Viar, J. Requies, Catalysts 10 (2020) 895, doi:http://dx.doi.org/10.3390/catal10080895.
[66] T. Buntara, I. Melián-Cabrera, Q. Tan, J.L.G. Fierro, M. Neurock, J.G. de Vries, H.J. Heeres, Catal. Today 210 (2013) 106, doi:http://dx.doi.org/10.1016/j.cattod.2013.04.012.
[67] J. He, S.P. Burt, M.R. Ball, I. Hermans, J.A. Dumesic, G.W. Huber, Appl. Catal. B Environ. 258 (2019) 117945, doi:http://dx.doi.org/10.1016/j.apcatb.2019.117945.
[68] S. Liu, Bioprocess Engineering: Kinetics, Sustainability, and Reactor Design, Elsevier, Amsterdam, 2017.
[69] M.A. Vannice, Kinetics of Catalytic Reactions, Springer, New York, 2005.
[70] C. Moreno-Marrodan, P. Barbaro, Green Chem. 16 (2014) 3434, doi:http://dx.doi.org/10.1039/C4GC00298A.
[71] A. Hommes, A.J. ter Horst, M. Koeslag, H.J. Heeres, J. Yue, Chem. Eng. J. 399 (2020) 125750, doi:http://dx.doi.org/10.1016/j.cej.2020.125750.
[72] W. Hao, W. Li, X. Tang, X. Zeng, Y. Sun, S. Liu, L. Lin, Green Chem. 18 (2016) 1080, doi:http://dx.doi.org/10.1039/c5gc01221j.
[73] S. Iqbal, S.A. Kondrat, D.R. Jones, D.C. Schoenmakers, J.K. Edwards, L. Lu, B.R. Yeo, P.P. Wells, E.K. Gibson, D.J. Morgan, C.J. Kiely, G.J. Hutchings, ACS Catal. 5 (2015) 5047, doi:http://dx.doi.org/10.1021/acscatal.5b00625.
[74] D. Albani, Q. Li, G. Vilé, S. Mitchell, N. Almora-Barrios, P.T. Witte, N. López, J. Pérez-Ramírez, Green Chem. 19 (2017) 2361, doi:http://dx.doi.org/10.1039/C6GC02586B.
[75] O.A. Abdelrahman, A. Heyden, J.Q. Bond, ACS Catal. 4 (2014) 1171, doi:http://dx.doi.org/10.1021/cs401177p.
[76] E.P. Maris, W.C. Ketchie, V. Oleshko, R.J. Davis, J. Phys. Chem. B 110 (2006) 7869, doi:http://dx.doi.org/10.1021/jp057022y.